This is a repository copy of *Discovery of ZZ Cetis in detached white dwarf plus main-sequence binaries*.

White Rose Research Online URL for this paper:
http://eprints.whiterose.ac.uk/108501/

Version: Accepted Version

Discovery of ZZ Cetis in detached white dwarf plus main-sequence binaries

S. Pyrzas[1]⋆, B. T. Gänsicke[2], J. J. Hermes[2], C. M. Copperwheat[3], A. Rebassa-Mansergas[4], V. S. Dhillon[5], S. P. Littlefair[5], T. R. Marsh[2], S. G. Parsons[6], C. D. J. Savoury[5], M. R. Schreiber[6], S. C. C. Barros[7], J. Bento[8], E. Breedt[2] and P. Kerry[5]

[1]*Instituto de Astronomía, Universidad Católica del Norte, Avenida Angamos 0610, Casilla 1280, Antofagasta, Chile*
[2]*Department of Physics, University of Warwick, Coventry, CV4 7AL, UK*
[3]*Astrophysics Research Institute, Liverpool John Moores University, Twelve Quays House, Birkenhead CH41 1LD, UK*
[4]*Kavli Institute for Astronomy and Astrophysics, Peking University, Beijing 100871, China*
[5]*Department of Physics and Astronomy, University of Sheffield, Sheffield S3 7RH, UK*
[6]*Departamento de Física y Astronomía, Universidad de Valparaíso, Avenida Gran Bretaña 1111, Valparaíso, Chile*
[7]*Aix Marseille Université, CNRS, LAM, UMR 7326, 13388, Marseille, France*
[8]*Department of Physics and Astronomy, Macquarie University, NSW 2109, Australia*

ABSTRACT

We present the first results of a dedicated search for pulsating white dwarfs (WDs) in detached white dwarf plus main-sequence binaries. Candidate systems were selected from a catalogue of WD+MS binaries, based on the surface gravities and effective temperatures of the WDs. We observed a total of 26 systems using ULTRACAM mounted on ESO's 3.5 m New Technology Telescope (NTT) at La Silla. Our photometric observations reveal pulsations in seven WDs of our sample, including the first pulsating white dwarf with a main-sequence companion in a post common envelope binary, SDSS J1136+0409. Asteroseismology of these new pulsating systems will provide crucial insight into how binary interactions, particularly the common envelope phase, affect the internal structure and evolution of WDs. In addition, our observations have revealed the partially eclipsing nature of one of our targets, SDSS J1223-0056.

Key words: stars: white dwarfs - stars: low-mass - binaries: close - binaries: eclipsing - asteroseismology

1 INTRODUCTION

The class of ZZ Ceti stars comprises single, hydrogen-atmosphere (DA), photometrically variable white dwarfs (WDs) (see e.g. McGraw 1977; Clemens 1993; Mukadam et al. 2006) that exhibit non-radial g-mode pulsations (Chanmugam 1972; Warner & Robinson 1972). ZZ Ceti stars are tightly grouped together in the *ZZ Ceti instability strip* (e.g. Bergeron et al. 1995; Koester & Allard 2000; Mukadam et al. 2004a; Gianninas et al. 2006; Van Grootel et al. 2012), a well defined region in the effective temperature ($T_{\rm eff}$)-surface gravity ($\log g$) plane, between 11,100 and 12,600 K for a $\log g = 8$ WD (Gianninas et al. 2011), with a dependence on $\log g$ (Giovannini et al. 1998). One of the fundamental questions regarding the instability strip is its assumed purity (e.g. Gianninas et al. 2005,

2006; Castanheira et al. 2010). While available evidence points to a pure strip (e.g. Bergeron et al. 1995, 2004; Castanheira et al. 2007), the purity has not yet been explicitly proved. A pure strip implies that ZZ Ceti-type pulsations are an evolutionary stage of all (single) DA white dwarfs[1] and thus, studies of ZZ Cetis can be applied to the entire population of DA white dwarfs. The means towards this end is asteroseismology.

Asteroseismology, the study of stellar pulsations, is a powerful tool to gather direct information about the interiors of stars. In the past few decades it has been successfully adapted to WDs to constrain the hydrogen layer mass,

---

⋆ E-mail: stylianos.pyrzas@gmail.com

[1] An impure strip doesn't necessarily imply the opposite. Impurities could arise if a third parameter is in effect, as is the case for cataclysmic variables, explained later in this Section. In such a case, the third parameter needs to be taken into account when defining the strip.

Table 1. Information on all our target WD+MS binaries. We provide names, coordinates, SDSS u, g, r magnitudes*, $T_{\rm eff}$, $\log g$ and $M_{\rm WD}$ values. The penultimate column gives the classification of each target (see text for details), while the last column gives the length of the observations.

SDSS J	RA [J2000]	Dec [J2000]	u	g	r	$T_{\rm eff}$ [a] [K]	$\log g$ [b]	$M_{\rm WD}$ [c] [M$_\odot$]	Class	Obs. Length [hrs]
0017-0024	00:17:26.63	-00:24:51.1	19.66	19.21	18.96	14594 ± 1487	7.96 ± 0.30	0.60 ± 0.18	WDMS	2.46
0021-1103	00:21:57.90	-11:03:31.6	19.22	18.57	18.10	11045 ± 164	8.78 ± 0.10	1.08 ± 0.05	WDMS	2.89
0052-0051	00:52:08.42	-00:51:34.6	19.04	18.30	17.72	12300 ± 427	8.46 ± 0.12	0.90 ± 0.08	WDMS	6.82[1]
0111+0009	01:11:23.89	+00:09:35.3	19.02	18.42	17.83	12321 ± 461	7.50 ± 0.25	0.37 ± 0.11	WDMS	2.85
0124-0023	01:24:03.11	-00:23:01.1	20.29	18.88	17.75	11972 ± 1509	6.70 ± 0.44	0.16 ± 0.10	WDMS	2.02
0203+0040	02:03:51.28	+00:40:25.1	20.32	19.43	18.67	10794 ± 475	8.17 ± 0.36	0.71 ± 0.22	WDMS	2.93
0212+0018	02:12:39.45	+00:18:56.9	19.69	19.22	18.87	13852 ± 2865	8.29 ± 0.47	0.79 ± 0.27	WDMS	2.48
0218+0057	02:18:49.98	+00:57:39.2	20.23	19.67	19.15	12250 ± 1007	7.46 ± 0.59	0.35 ± 0.29	UNKN	2.63
0255-0044	02:55:09.29	-00:44:14.7	20.76	19.69	18.74	13182 ± 1916	7.41 ± 0.61	0.36 ± 0.27	WDMS	2.71
0327-0022	03:27:58.15	-00:22:15.4	20.47	19.48	18.63	12902 ± 874	7.80 ± 0.31	0.50 ± 0.17	WDMS	3.17
0328+0017	03:28:42.92	+00:17:49.7	19.06	18.03	16.16[2]	12504 ± 514	7.56 ± 0.15	0.40 ± 0.07	WDMS	2.39
0336-0047	03:36:56.12	-00:47:27.8	20.09	19.49	19.23	15246 ± 1042	7.79 ± 0.24	0.50 ± 0.13	WDMS	3.10
0345-0614	03:45:14.71	-06:14:21.2	20.16	19.31	18.51	13904 ± 1267	8.24 ± 0.27	0.76 ± 0.17	PCEB	3.61
0824+1723[3]	08:24:29.02	+17:23:45.4	19.06	18.34	17.83	11433 ± 358	8.21 ± 0.18	0.74 ± 0.12	WDMS	2.52
1043+0603[4]	10:43:58.59	+06:03:20.9	19.24	18.75	18.78	11173 ± 299	8.19 ± 0.20	0.72 ± 0.13	WDMS	2.73
1054+1008	10:54:36.18	+10:08:37.3	18.98	18.61	18.58	11433 ± 229	7.97 ± 0.13	0.59 ± 0.09	UNKN	1.87
1117-1255	11:17:10.54	-12:55:40.9	20.30	19.65	19.25	11302 ± 357	8.29 ± 0.24	0.79 ± 0.15	WDMS	1.18
1136+0409	11:36:55.17	+04:09:52.6	17.57	17.07	17.17	11699 ± 152	7.99 ± 0.08	0.60 ± 0.05	PCEB	1.05
1223-0056	12:23:39.61	-00:56:31.2	18.41	17.91	18.06	11565 ± 159	7.71 ± 0.11	0.45 ± 0.06	PCEB[5]	7.75[6]
1228-0225	12:28:50.46	-02:25:09.4	20.74	19.61	18.52	13127 ± 6398	8.96 ± 0.73	1.18 ± 0.38	WDMS	1.62
1329+2557	13:29:33.67	+25:57:43.2	20.09	18.75	17.75	11565 ± 1177	8.43 ± 0.44	0.88 ± 0.26	UNKN	0.71
1453+0010	14:53:05.77	+00:10:48.2	19.71	18.90	18.21	11565 ± 233	8.55 ± 0.09	0.95 ± 0.05	WDMS	1.93
1520+0634	15:20:33.43	+06:34:42.9	19.47	18.91	18.52	11302 ± 234	8.47 ± 0.12	0.86 ± 0.09	WDMS	1.39
1615+2357	16:15:05.51	+23:57:46.3	19.02	18.23	17.66	12250 ± 595	8.11 ± 0.12	0.67 ± 0.08	UNKN	1.99
1652+1340	16:52:40.74	+13:40:15.0	20.95	19.98	19.11	11173 ± 101	8.44 ± 0.44	0.88 ± 0.25	UNKN	1.31
1724+0733	17:24:45.28	+07:33:24.7	19.51	18.86	18.35	13588 ± 527	8.02 ± 0.12	0.62 ± 0.08	WDMS	1.85

* These magnitudes are on the SDSS 2.5 m photometric system. Note, however, that ULTRACAM filters are primed,
  i.e. u', g', r', i', as they are closer to the USNO 40-in system (Fukugita et al. 1996; Smith et al. 2002).
[a,b,c] Values obtained using the updated spectral decomposition/fitting technique described in detail in Rebassa-Mansergas et al. (2012).
[1] Total time over two observing nights ; [2]This is an i magnitude, and the system was observed in the i'-band ; [3]Exposure time for
u'-band was 40 sec ; [4]Exposure time for all bands was 10 sec ; [5]Originally mis-classified as a WDMS, see Sec. 4.1 ; [6]Total time

the depth of the degenerate core boundary, the overall stellar mass and temperature, the mass of any other chemically stratified layers, and the rotation rates of these stellar remnants (Winget & Kepler 2008; Fontaine & Brassard 2008; Althaus et al. 2010).

As the end-point of all low-mass stars, WDs are also frequently found in binary configurations, such as cataclysmic variables (CVs), close interacting binaries in which the WD primary accretes from a low-mass companion. With the discovery of ZZ Ceti-type pulsations in the WD primary of the CV GW Lib (Warner & van Zyl 1998; van Zyl et al. 2000, 2004), the analytic power of asteroseismology has become available to determine accurate stellar parameters for the WDs in these binaries, which is otherwise very difficult, if not impossible, to achieve, as the light from the WD is contaminated with emission from the accretion disc. Asteroseismology also offers the opportunity to study how the accretion of mass and angular momentum onto the WDs in CVs can affect the WD structure, shedding light on the potential single-degenerate scenario for SN Type-Ia progenitors. Most of the (non-magnetic) WDs in CVs were not expected to be pulsating, as accretion heats them to effective temperatures greater than 12000 K (Townsley & Gänsicke 2009). The work of Townsley et al. (2004) and Arras et al. (2006) suggested that the atmospheric composition of accreting WDs, especially the He abundance, the accretion of

heavier elements and the rapid rotation of the WD primaries in CVs could significantly affect the pulsation modes. There are currently 16 known pulsating WDs in CVs. Most of them show a single pulsation mode, and thus it has not been possible to derive stellar parameters through asteroseismology for any of them. Their corresponding instability strip seems to be wider than the one for non-interacting ZZ Cetis, ranging from $10500\,{\rm K} \lesssim T_{\rm eff} \lesssim 16000\,{\rm K}$ (Szkody et al. 2010, and references therein), although this result is based on small-number statistics. However, its location as derived from observations is consistent with theoretical expectations (e.g. Arras et al. 2006), for a high He abudance (> 0.48). We should note that the CV strip is not pure, most likely a consequence of the 3-dimensional parameter space, with the He abundance as the third parameter, in addition to $T_{\rm eff}$ and $\log g$.

The occurrence of pulsating WDs in CVs raises the question of the existence of pulsating WDs in the progenitors of CVs and, generally, in non-interacting binaries, such as detached white dwarf plus main-sequence binaries (WD+MS). In recent years, owing mainly to the Sloan Digital Sky Survey (SDSS, York et al. 2000), WD+MS binaries have been discovered in large numbers (e.g. Silvestri et al. 2005; Heller et al. 2009; Rebassa-Mansergas et al. 2010, 2012; Liu et al. 2012; Rebassa-Mansergas et al. 2013), offering the exciting possibility for ensemble asteroseismology

studies of a large and homogeneous sample of WDs in binaries.

About two-thirds of the SDSS WD+MS binaries are wide enough that the WD progenitors have evolved as if they were single stars (e.g. Willems & Kolb 2004; Schreiber et al. 2010; Nebot Gómez-Morán et al. 2011). Thus, pulsating WDs in such systems should exhibit properties very similar to the single ZZ Cetis. This hypothesis remains effectively untested by observations; to our knowledge, there is only one confirmed ZZ Ceti in a wide common proper motion binary, G117-B15A (e.g. Kepler et al. 1991).

The rest of the WD+MS binaries are expected to be post-common envelope binaries (PCEBs), i.e. close binaries that have formed through common envelope (CE) evolution (e.g. Webbink 2008, for a review). The CE phase is believed to be the main mechanism for the formation of low mass, He-core WDs (e.g Paczynski 1976; Iben & Tutukov 1986).

While the presence of such WDs in PCEBs has been established observationally, in both double-degenerate (Marsh et al. 1995; Marsh 1995; Steinfadt et al. 2010; Parsons et al. 2011; and see also Nelemans & Tout 2005 and references therein) and single-degenerate (i.e. with a MS companion) configurations (Marsh & Duck 1996; Bruch 1999; Pyrzas et al. 2012; Parsons et al. 2012 and see also Schreiber & Gänsicke 2003 and references therein), pulsating He-core WDs have resisted detection (Steinfadt et al. 2012) and have been discovered only very recently, in double-degenerate configurations (extremely low mass WDs (ELM), Hermes et al. 2012, 2013b,a). Previous to our work, no pulsating WDs in single-degenerate PCEBs were known.

The study of pulsating WDs in PCEBs can provide crucial insight into whether, and if so how, the internal structure of WDs, and by extension the pulsation properties, are affected by the common envelope phase. White dwarfs in single-degenerate PCEBs can be found mainly in two "flavours", those with $M_{\rm WD} < 0.45\,{\rm M_\odot}$ and a He-core and those with $M_{\rm WD} \geqslant 0.5\,{\rm M_\odot}$ and a C/O core (e.g. Pyrzas et al. 2009; Rebassa-Mansergas et al. 2011); the juxtaposition of the two classes can provide fertile ground for studies on the potential effects of mass loss on the WD structure and pulsations. Furthermore, these systems can populate the gap in WD mass between the normal ZZ Cetis (with $M_{\rm WD} = 0.6\,{\rm M_\odot}$ and above) and the ELMs (with $M_{\rm WD} < 0.25\,{\rm M_\odot}$), leading to a complete census of pulsating WDs.

In this paper we present the first results from a dedicated search for pulsating WDs in WD+MS binaries. The structure is as follows: our target selection, photometric observations and period analysis techniques are described in Sec. 2 and 3 respectively, while Section 4 presents our results. We discuss our findings in Sec. 5 and conclude in Sec. 6 with a summary and suggestions for future work.

2 TARGET SELECTION

Targets were selected from the white dwarf plus main-sequence binaries catalogue by Rebassa-Mansergas et al. (2012). Systems were chosen on the basis of their $\log g$ and $T_{\rm eff}$ values, as determined from their SDSS spectra, using the spectral decomposition/fitting technique described in detail in Rebassa-Mansergas et al. (2007) (and see also

Rebassa-Mansergas et al. 2012). Table 1 lists basic information on all our targets and the observations. Based on available radial velocity (RV) information, either from the original SDSS spectroscopy or from follow-up observations, these 26 targets can be divided into three groups:

(i) PCEB: systems for which spectroscopy reveals radial velocity variations (close binaries)
(ii) WDMS: systems for which spectroscopy reveals no radial velocity variations (wide binary candidates)
(iii) UNKN: systems for which no or insufficient spectroscopy is available

While the detection of short period RV variations unambiguously identifies the PCEBs among our targets, the absence of RV variations is not a guarantee that a system is a wide binary. Insufficient spectral resolution, low orbital inclination or an unlucky orbital phase sampling can prevent the identification of a PCEB (see e.g. Schreiber et al. 2010, for a discussion). An example is SDSS J1223-0056, whose available spectroscopy did not show any RV variations and the system was classified as a WDMS. However, our subsequent photometric observations revealed the system to be eclipsing (see Sec. 4.1); the orbital period was determined to be $P_{\rm orb} = 2.2\,{\rm h}$, unambiguously re-classifying the system as a PCEB. Thus, WDMS should be read as "candidate wide WD+MS binary."

3 OBSERVATIONS, REDUCTIONS AND ANALYSIS

3.1 Photometry: NTT/ULTRACAM

Photometric light curves of our targets were obtained during two observing runs in December 2010 and May 2011. We used the high-speed camera ULTRACAM (Dhillon et al. 2007) mounted as a visitor instrument on ESO's 3.5 m New Technology Telescope (NTT) at La Silla Observatory, Chile. Each target was observed in full-frame mode, for a continuous block of time, but varying in length depending on the schedule. The exposure time was 20 s, with a dead-time between exposures of $\sim 25\,{\rm ms}$. ULTRACAM is a triple-beam camera, so data were obtained simultaneously in the Sloan u', g' and r' bands. In one case an i' filter was used instead of r' for scheduling reasons. All of the data were reduced with aperture photometry using the ULTRACAM pipeline software, with debiasing, flat-fielding and sky background subtraction performed in the standard way. The fluxes of the targets were determined using a variable aperture, whereby the radius of the aperture is scaled according to the full width at half-maximum of the stellar profile. Variations in transparency were accounted for by dividing each light curve by the light curve of a nearby comparison star. The stability of these comparison stars was checked against other stars in the field, and no variations were seen.

3.2 Period analysis

For the period analysis and the detection of pulsations, each light curve was first converted into fractional intensity (dividing by the mean and subtracting 1). Subsequently,

Table 2. Summary of the pulsation properties of the seven ZZ Ceti white dwarfs. We provide the frequency, the corresponding period and the amplitude of each detection for all three ULTRACAM arms, as well as the corresponding detection thresholds. A dash indicates no detection.

System SDSS J	Frequency [μHz] u'	g'	r'	Period [s] u'	g'	r'	Amplitude [mma[1]] u'	g'	r'	Det. Thresh. [mma] u'	g'	r'
0052-0051[2]	-	928.36 ± 12.73	932.18 ± 9.84	-	1077.2 ± 14.8	1072.8 ± 11.3	-	4.0	2.4	30.8	2.7	2.2
	-	914.24 ± 5.21	-	-	1093.8 ± 6.2	-	-	4.0	-	32.3	2.5	2.2
0111+0009	1130.94 ± 8.30	1131.68 ± 8.15	1134.34 ± 17.55	884.2 ± 6.5	883.6 ± 6.4	881.6 ± 13.6	33.2	15.9	6.2	22.0	9.0	4.5
	1579.63 ± 7.87	1583.34 ± 4.51*	1581.13 ± 5.21	633.1 ± 3.2	631.6 ± 1.8	632.5 ± 2.1	40.2	28.0	10.1	22.0	9.0	4.5
	1715.74 ± 9.49	1714.58 ± 5.21	1704.75 ± 7.06	582.8 ± 3.2	583.2 ± 1.8	586.6 ± 2.4	21.4	16.3	6.3	22.0	9.0	4.5
	1950.12 ± 8.45	1960.07 ± 5.44	1955.56 ± 8.10	512.8 ± 2.2	510.2 ± 1.4	511.4 ± 2.1	25.5	18.9	7.7	22.0	9.0	4.5
	-	2728.59 ± 14.47	2723.26 ± 12.85[a]	-	366.5 ± 1.9	367.2 ± 1.7	-	9.1	4.4	22.0	9.0	4.5
0203+0040	1039.24 ± 7.87	1044.91 ± 2.78*	1049.77 ± 4.40	962.4 ± 7.3	957.0 ± 2.6	952.6 ± 4.0	70.8	38.5	11.7	46.2	8.5	4.7
	1456.48 ± 10.19[a]	1462.26 ± 7.41	1483.91 ± 9.14	685.9 ± 4.8	683.9 ± 3.5	673.9 ± 4.2	41.8	15.2	4.8	46.2	8.5	4.7
	-	2507.75 ± 8.56	2510.30 ± 11.69	-	398.8 ± 1.4	398.4 ± 1.9	-	11.9	4.7	46.2	8.5	4.7
0824+1723	1010.88 ± 11.34	1012.26 ± 8.91	1031.48 ± 7.18	989.2 ± 11.1	987.9 ± 8.7	969.5 ± 6.7	27.3	12.0	6.7	25.1	7.5	4.3
	1178.82 ± 14.58	1238.88 ± 10.30	1190.16 ± 11.92	848.3 ± 10.5	807.2 ± 6.7	840.2 ± 8.4	29.2	13.9	5.7	25.1	7.5	4.3
	1313.77 ± 17.82	-[b]	1300.12 ± 19.33	761.2 ± 10.3	-	769.2 ± 11.4	28.6	-	4.6	25.1	7.5	4.3
	1588.43 ± 14.35	1603.47 ± 4.75*	1626.97 ± 11.69	629.6 ± 5.7	623.7 ± 1.9	614.7 ± 4.4	30.4	20.4	7.5	25.1	7.5	4.3
	-	1945.60 ± 9.83	1967.36 ± 11.11	-	513.9 ± 2.6	508.3 ± 2.9	-	9.2	4.7	28.0	7.5	4.3
1043+0603	-	1576.27 ± 6.71	1567.71 ± 11.69	-	634.4 ± 2.7	637.9 ± 4.8	-	8.5	7.1	24.6	4.5	5.8
	-	3080.21 ± 2.20*	3082.06 ± 3.70	-	324.7 ± 0.2	324.6 ± 0.4	-	28.8	18.3	24.6	4.5	5.8
	-	3419.10 ± 15.97	-	-	292.5 ± 1.4	-	-	5.3	-	24.6	4.5	5.8
	-	6167.94 ± 7.52†	6143.52 ± 18.63[a]	-	164.9 ± 0.2	162.8 ± 0.5	-	6.6	5.5	24.6	4.5	5.8
1117-1255	-	1196.53 ± 15.51*	1248.26 ± 18.87[a]	-	835.80 ± 10.80	801.10 ± 12.10	-	21.9	13.1	77.2	10.9	13.6
1136+0409	-	3616.67 ± 13.31*	3656.37 ± 17.36	-	276.5 ± 1.0	273.5 ± 1.3	-	8.3	6.3	22.1	3.6	4.9
	-	5489.70 ± 19.91	-	-	182.2 ± 0.7	-	-	4.4	-	22.1	3.6	4.9

[1] mma: milli-modulation amplitude, a 0.1% relative amplitude change ; [2] Two observations - solution for each independent observation
* Pre-whitened signal ; [a] Only $> 2\sigma$ detection ; [b] Barely 1σ detection ; † First harmonic of the 3080.21 signal
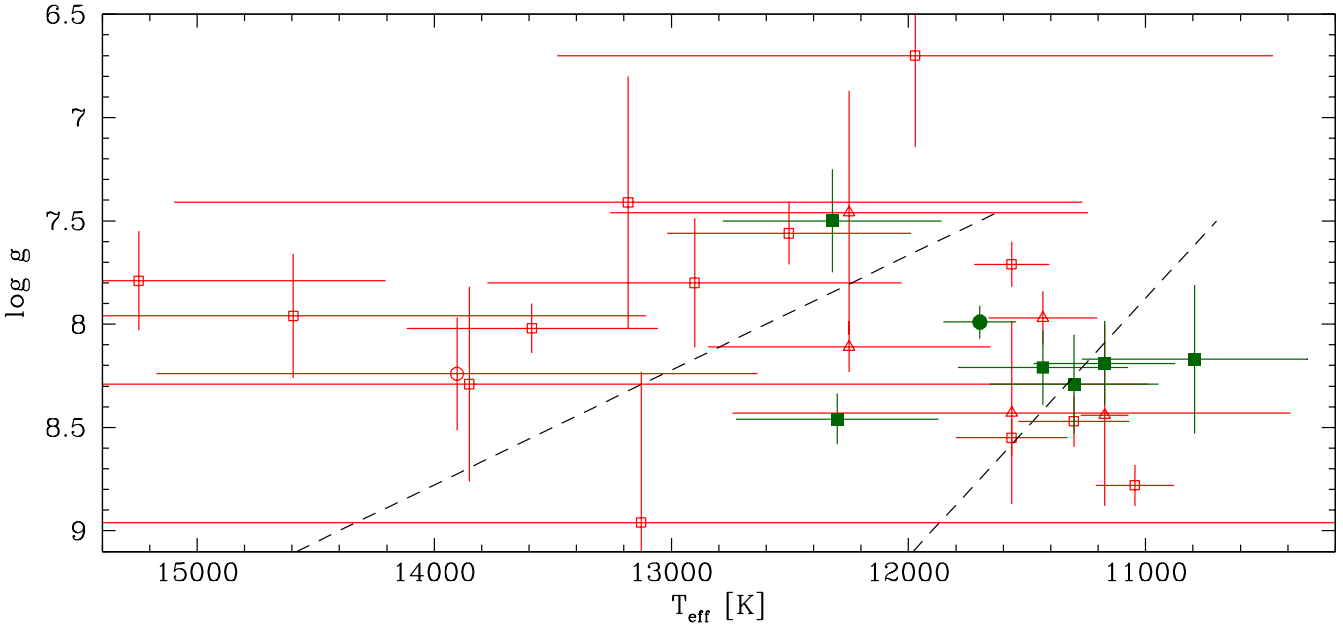
Figure 1. The results of our campaign. The 26 systems plotted on the $T_{\rm eff}$ - $\log g$ plane. Pulsating systems are shown with green, filled symbols; non-pulsating systems with red, open symbols (colour version available only online). Circles denote PCEB, squares WDMS and triangles UNKN binaries, following Table 1. The dashed lines are the boundaries of the ZZ Ceti instability strip found by Gianninas et al. (2011).
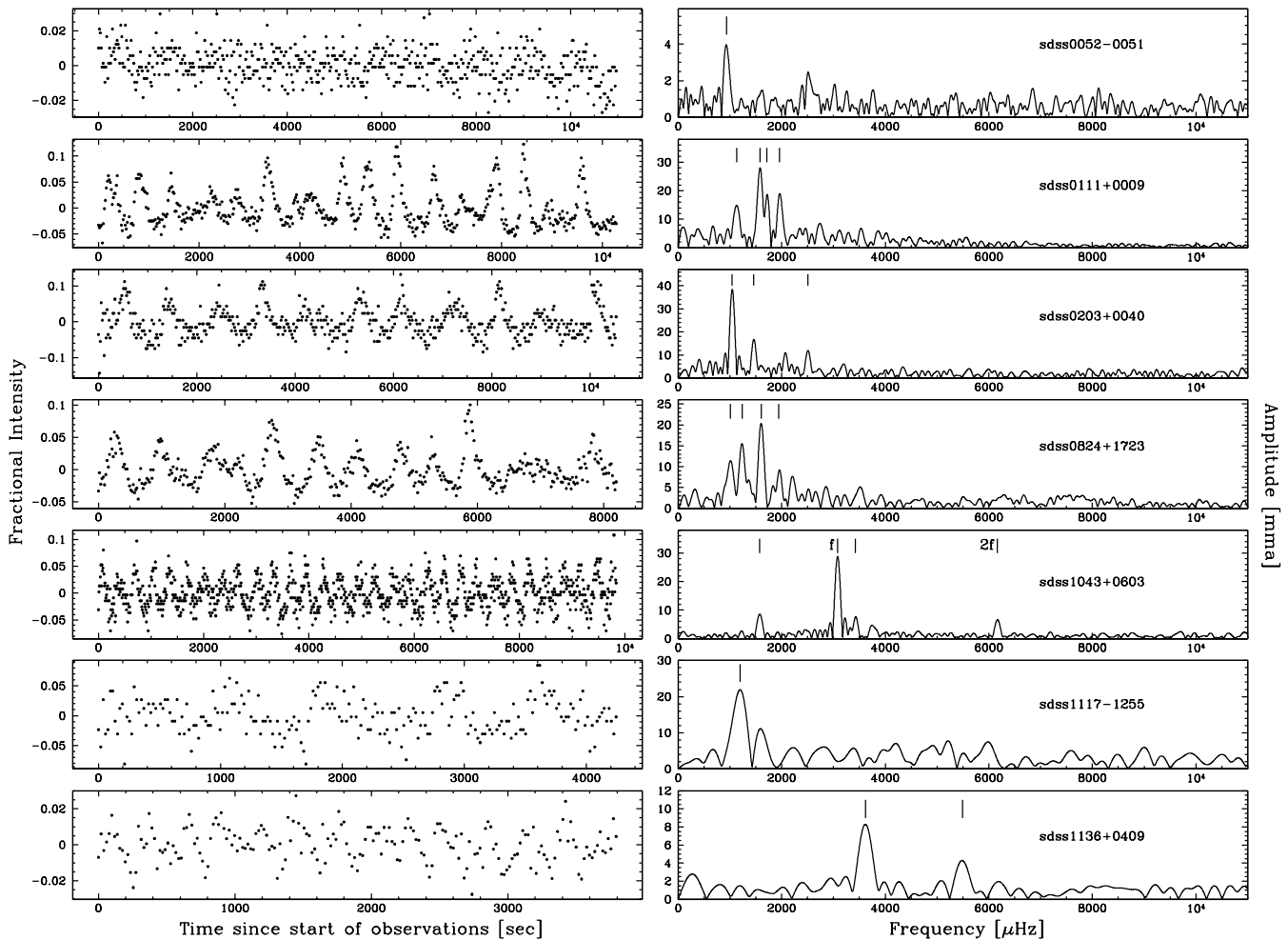
Figure 2. The seven pulsating WDs: g'-band light curves (left panels) and the corresponding amplitude spectra (right panels) for each system, identified in the right panels. Tickmarks indicate the significant detections for each system, as listed in Table 2.

we calculated amplitude spectra using the TSA package (Schwarzenberg-Czerny 1993) as implemented in `MIDAS`.

In order to judge the significance of a signal, we calculated a detection threshold in the following fashion (see also Greiss et al. 2014): for each light curve we created artificial data sets using a shuffling technique (see e.g. Kepler 1993; Schreiber 2007, for discussions), where each intensity point f_i is randomly re-assigned to a time point t_j with $i \neq j$; all intensity and time points are used. This shuffling destroys any coherent signal, but retains the time- and overall noise properties of a light curve. We then calculated the amplitude spectra of the shuffled light curves and recorded the value of highest amplitude. Using the results from 10,000 shufflings, we calculated the amplitudes corresponding to the 68.3, 95.5 and 99.7 per cent confidence levels (1-, 2- and 3-σ respectively) and set the 3σ amplitude as our detection threshold. Signals with amplitudes above this threshold were considered significant. Finally, the frequencies and errors of significant detections were determined using the bootstrap method (Press 2002).

When strong signals are present, using the maximum amplitude to determine the threshold typically leads to overestimated threshold values. Therefore, our analysis was carried out as follows: for each light curve, we used our shuffling technique to calculate the detection threshold and to ensure that the strongest signal present in the power spectrum is indeed a 3-σ detection. Subsequently, we prewhitened this signal, and subjected the light curve to a second shuffling, in order to calculate the revised detection threshold and look for additional significant signals. We did not proceed with further iterations, as we have only one relatively short light curve per target.

4 RESULTS

Our photometric observations and subsequent period analysis revealed the pulsating nature of seven white dwarfs in our sample, while the remaining 19 were found to be nonvariable at our detection threshold. Our results are illustrated in Figure 1.

Table 2 lists the seven systems with $> 3\sigma$ signal detections, along with the corresponding frequencies, periods, amplitudes and detection thresholds in each filter, while Fig. 2 shows the g'-band light curves and the corresponding amplitude spectra of all seven pulsating systems.

In Table 3 we list all the non-pulsating systems along with the corresponding detection thresholds in each of the
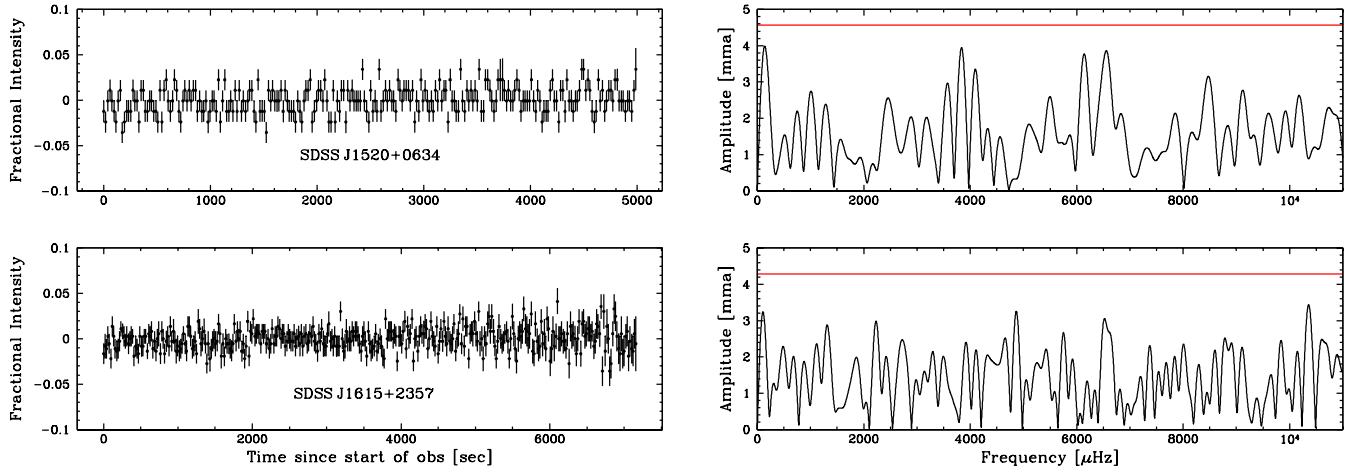
Figure 3. Sample g'-band light curves (left panels) and their corresponding amplitude spectra (right panels) of two of our non-pulsating WDs, SDSS J1520+0634 (top panels) and SDSS J1615+2357 (bottom panels). Red lines indicate the 3σ detection threshold.

Table 3. Detection thresholds for the 19 white dwarfs where no pulsations were detected.

System	Threshold [mma]		
SDSS J	u'	g'	r'
0017-0024	21.3	4.4	5.5
0021-1103	14.4	3.3	3.4
0124-0023	38.5	4.2	2.5
0212+0018	19.9	4.1	4.5
0218+0057	94.6	21.7	10.9
0255-0044	62.6	10.2	4.8
0327-0022	72.4	9.6	6.7
0328+0017	51.7	5.2	1.2
0336-0047	30.2	6.3	5.67
0345-0614	54.3	8.2	4.2
1054+1008	50.2	10.1	15.5
1223-0056	9.7	2.1	3.1
1228-0225	217.2	26.0	13.9
1329+2557	87.0	8.3	6.2
1453+0010	25.6	4.1	3.3
1520+0634	22.5	4.6	5.1
1615+2357	33.5	4.3	4.6
1652+1340	92.6	13.8	9.3
1724+0733	36.5	6.3	7.4

three filters, while Fig. 3 shows two sample g'-band light curves and their respective amplitude spectra.

The periods observed in our systems are comparable to those observed in typical pulsating WDs (e.g. Mukadam et al. 2006). All our systems are detached, so we do not expect to see any accretion-related variability, such as flickering and QPO's. In detached systems, photometric variability could be caused by ellipsoidal modulation or irradiation/reflection effects (see e.g. Pyrzas et al. 2009; Parsons et al. 2010). However, these forms of variability are modulated on longer timescales (effectively on the orbital period, with two maxima and one maximum per orbit respectively) than the periods observed in our sample, and have a distinctive qualitative imprint on the light curves, very different to the observed variability. Henceforth, we will *assume* that each $> 3\sigma$ detection corresponds to a pulsa-
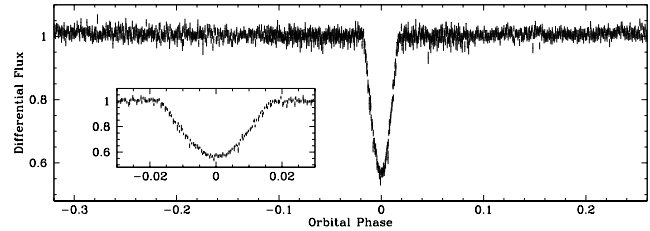
Figure 4. Phase-folded g'-band lightcurve of SDSS J1223-0056, using the orbital ephemeris Eq. 1. Inset panel: a zoom-in version around the eclipse itself.

tion mode, although repeated detections of each pulsation would be required for unambiguous confirmation.

4.1 SDSS J1223-0056

Our photometric observations revealed that the white dwarf in SDSS J1223-0056 undergoes partial eclipses. Measuring the times of mid-eclipse from four observed eclipses, we determine the orbital ephemeris of the system to be

$$\mathrm{BMJD}_0(\mathrm{TDB}) = 55706.11231(1) + E * 0.0900844(9) \quad (1)$$

that is $P_{\mathrm{orb}} = 2.16202(2)$ [h], where the numbers in brackets indicate the error on the last digit. Figure 4 shows a phase-folded g'-band lightcurve of the new eclipsing system. SDSS J1223-0056 has also been detected as an eclipsing system in data from the Catalina Real-time Transient Survey (see Parsons et al. 2013).

5 DISCUSSION

Inspection of Tab. 2 and 3 reveals that in the majority of cases, our u'-band detection threshold is much higher than the g'- and r'-band, since the quality of the data in this band is compromised by the faintness of the targets and the lack of good comparison stars in the fields. As a result, in some of the pulsating systems there is no u'-band detection of the pulsations, although the respective g'- and r'-band detections are unambiguous.

Our survey for pulsations generally has a relatively low sensitivity; the median value for WDs not observed to vary is 6.3 mma in the g'-band, only slightly below the median amplitude of 8.8 mma for detected pulsations in a sample of 35 ZZ Cetis discovered from SDSS (Mukadam et al. 2004b). Pulsation signals could also be diluted if the M-dwarf companion contributes a significant amount of flux. Thus, it is possible that we might have missed some pulsators among these seemingly non-variable systems.

For our seven pulsating systems, the frequencies of the detected signals are consistent with those of g-mode pulsations observed in single WDs (e.g. Mukadam et al. 2006). The multicolour amplitudes of the pulsations (particularly in the cases where u'-band pulsations are also detected) are indicative of $\ell = 1, 2$ modes (Robinson et al. 1995). Three systems (SDSS J0111+0009, J0824+1723 and J1043+0603, all of them wide WDMS candidates) show multiple pulsation periods, making them promising candidates for intensive follow-up asteroseismic studies. Among the three confirmed PCEBs in our sample, only SDSS J1136+0409 is pulsating, while J1223-0056 and J0345-0614 show no pulsations at our detection limit.

Finally, we note that if we take the $T_{\rm eff}$ and $\log g$ of these WDs at face value, two of our pulsating systems (SDSS J0111+0009 and J0203+0040) lie nominally outside the Gianninas et al. (2011) instability strip, while six systems with no detections lie inside it. However, it is important to bear in mind that the parameters determined from the spectral decomposition (Rebassa-Mansergas et al. 2010, 2012) have rather large statistical errors (evident in the errors bars of Fig. 1) and can be subject to systematic uncertainties (see Parsons et al. 2013). In WD+MS binaries, the subtraction of the M-dwarf component from the spectrum directly affects the disambiguation between the "hot" and "cold" solutions of the subsequent WD fit. It is possible that for some of our systems we have selected the "wrong" solution. Also, $\log g$ values are overestimated for those systems with $T_{\rm eff} < 12000$ K, when using 1-dimensional WD models to perform the fits. Recently Tremblay et al. (2013) published 3-dimensional WD models, allowing for corrections to the 1D $\log g$ values. However, since these 3D corrections have not yet been implemented in the context of an empirical ZZ Ceti instability strip, we have not adopted them in our analysis.

6 CONCLUSIONS

We have carried out the first dedicated survey to identify pulsating white dwarfs in detached WD+MS binaries. Among a sample of 26 such systems, selected based on the $T_{\rm eff}$ and $\log g$ values of their WDs obtained from spectral fitting, we have idenified seven new pulsating white dwarfs. One of these WDs is found in SDSS J1136+0409, a confirmed single-degenerate post-common-envelope binary, which constitutes the first detection of such kind.

For the immediate future, work needs to be carried out on multiple fronts: (i) high signal-to-noise spectroscopy of all our targets with wide wavelentgh coverage (across the Balmer jump) in order to pinpoint their exact location on the $T_{\rm eff}$ - $\log g$ plane, (ii) higher signal-to-noise photometric time series of the seemingly non-variable systems and (iii) follow-up photometric observations of all pulsating WDs in order to identify candidates for precision asteroseismology.

REFERENCES

Althaus, L. G., Córsico, A. H., Isern, J., García-Berro, E., 2010, A&AR, 18, 471
Arras, P., Townsley, D. M., Bildsten, L., 2006, ApJ Lett., 643, L119
Bergeron, P., Wesemael, F., Lamontagne, R., Fontaine, G., Saffer, R. A., Allard, N. F., 1995, ApJ, 449, 258
Bergeron, P., Fontaine, G., Billères, M., Boudreault, S., Green, E. M., 2004, ApJ, 600, 404
Bruch, A., 1999, AJ, 117, 3031
Castanheira, B. G., Kepler, S. O., Kleinman, S. J., Nitta, A., Fraga, L., 2010, MNRAS, 405, 2561
Castanheira, B. G., et al., 2007, A&A, 462, 989
Chanmugam, G., 1972, Nat, 236, 83
Clemens, J. C., 1993, Baltic Astronomy, 2, 407
Dhillon, V. S., et al., 2007, MNRAS, 378, 825
Fontaine, G., Brassard, P., 2008, PASP, 120, 1043
Fukugita, M., Ichikawa, T., Gunn, J. E., Doi, M., Shimasaku, K., Schneider, D. P., 1996, AJ, 111, 1748
Gianninas, A., Bergeron, P., Fontaine, G., 2005, ApJ, 631, 1100
Gianninas, A., Bergeron, P., Fontaine, G., 2006, AJ, 132, 831
Gianninas, A., Bergeron, P., Ruiz, M. T., 2011, ApJ, 743, 138
Giovannini, O., Kepler, S. O., Kanaan, A., Wood, A., Claver, C. F., Koester, D., 1998, BaltA, 7, 131
Greiss, S., Gänsicke, B. T., Hermes, J. J., Steeghs, D., Koester, D., Ramsay, G., Barclay, T., Townsley, D. M., 2014, MNRAS, 438, 3086
Heller, R., Homeier, D., Dreizler, S., Østensen, R., 2009, A&A, 496, 191
Hermes, J. J., Montgomery, M. H., Winget, D. E., Brown, W. R., Kilic, M., Kenyon, S. J., 2012, ApJ Lett., 750, L28

Hermes, J. J., et al., 2013a, MNRAS, 436, 3573

Hermes, J. J., et al., 2013b, ApJ, 765, 102

Iben, Jr., I., Tutukov, A. V., 1986, ApJ, 311, 742

Kepler, S. O., 1993, BaltA, 2, 515

Kepler, S. O., et al., 1991, ApJ Lett., 378, L45

Koester, D., Allard, N. F., 2000, BaltA, 9, 119

Liu, C., Li, L., Zhang, F., Zhang, Y., Jiang, D., Liu, J., 2012, MNRAS, 424, 1841

Marsh, T. R., 1995, MNRAS, 275, L1

Marsh, T. R., Duck, S. R., 1996, MNRAS, 278, 565

Marsh, T. R., Dhillon, V. S., Duck, S. R., 1995, MNRAS, 275, 828

McGraw, J. T., 1977, The ZZ Ceti stars: A new class of pulsating white dwarfs, Ph.D. thesis, Texas Univ., Austin.

Mukadam, A. S., Winget, D. E., von Hippel, T., Montgomery, M. H., Kepler, S. O., Costa, A. F. M., 2004a, ApJ, 612, 1052

Mukadam, A. S., Montgomery, M. H., Winget, D. E., Kepler, S. O., Clemens, J. C., 2006, ApJ, 640, 956

Mukadam, A. S., et al., 2004b, ApJ, 607, 982

Nebot Gómez-Morán, A., et al., 2011, A&A, 536, A43

Nelemans, G., Tout, C. A., 2005, MNRAS, 356, 753

Paczynski, B., 1976, in P. Eggleton, S. Mitton, & J. Whelan, ed., Structure and Evolution of Close Binary Systems, vol. 73 of *IAU Symposium*, p. 75

Parsons, S. G., Marsh, T. R., Copperwheat, C. M., Dhillon, V. S., Littlefair, S. P., Gänsicke, B. T., Hickman, R., 2010, MNRAS, 402, 2591

Parsons, S. G., Marsh, T. R., Gänsicke, B. T., Drake, A. J., Koester, D., 2011, ApJ Lett., 735, L30

Parsons, S. G., et al., 2012, MNRAS, 420, 3281

Parsons, S. G., et al., 2013, MNRAS, 429, 256

Press, W. H., 2002, Numerical recipes in C++ : the art of scientific computing, Cambridge Univ. Press, Cambridge

Pyrzas, S., et al., 2009, MNRAS, 394, 978

Pyrzas, S., et al., 2012, MNRAS, 419, 817

Rebassa-Mansergas, A., Gänsicke, B. T., Rodríguez-Gil, P., Schreiber, M. R., Koester, D., 2007, MNRAS, 382, 1377

Rebassa-Mansergas, A., Gänsicke, B. T., Schreiber, M. R., Koester, D., Rodríguez-Gil, P., 2010, MNRAS, 402, 620

Rebassa-Mansergas, A., Nebot Gómez-Morán, A., Schreiber, M. R., Girven, J., Gänsicke, B. T., 2011, MNRAS, 413, 1121

Rebassa-Mansergas, A., Nebot Gómez-Morán, A., Schreiber, M. R., Gänsicke, B. T., Schwope, A., Gallardo, J., Koester, D., 2012, MNRAS, 419, 806

Rebassa-Mansergas, A., Agurto-Gangas, C., Schreiber, M. R., Gänsicke, B. T., Koester, D., 2013, MNRAS, 433, 3398

Robinson, E. L., et al., 1995, ApJ, 438, 908

Schreiber, M. R., 2007, A&A, 466, 1025

Schreiber, M. R., Gänsicke, B. T., 2003, A&A, 406, 305

Schreiber, M. R., et al., 2010, A&A, 513, L7

Schwarzenberg-Czerny, A., 1993, in P. Grosbol & R. de Ruijsscher, ed., 5. ESO/ST-ECF Data Analysis Workshop, vol. 47 of *ESO Conference and Workshop Proceedings*, p. 149

Silvestri, N. M., Hawley, S. L., Oswalt, T. D., 2005, AJ, 129, 2428

Smith, J. A., et al., 2002, AJ, 123, 2121

Steinfadt, J. D. R., Kaplan, D. L., Shporer, A., Bildsten, L., Howell, S. B., 2010, ApJ Lett., 716, L146

Steinfadt, J. D. R., Bildsten, L., Kaplan, D. L., Fulton, B. J., Howell, S. B., Marsh, T. R., Ofek, E. O., Shporer, A., 2012, PASP, 124, 1

Szkody, P., et al., 2010, ApJ, 710, 64

Townsley, D. M., Gänsicke, B. T., 2009, ApJ, 693, 1007

Townsley, D. M., Arras, P., Bildsten, L., 2004, ApJ Lett., 608, L105

Tremblay, P.-E., Ludwig, H.-G., Steffen, M., Freytag, B., 2013, A&A, 559, A104

Van Grootel, V., Dupret, M.-A., Fontaine, G., Brassard, P., Grigahcène, A., Quirion, P.-O., 2012, A&A, 539, A87

van Zyl, L., Warner, B., O'Donoghue, D., Sullivan, D., Pritchard, J., Kemp, J., 2000, BaltA, 9, 231

van Zyl, L., et al., 2004, 350, 307

Warner, B., Robinson, E. L., 1972, Nat, 239, 2

Warner, B., van Zyl, L., 1998, in F.-L. Deubner, J. Christensen-Dalsgaard, & D. Kurtz, ed., New Eyes to See Inside the Sun and Stars, vol. 185 of *IAU Symposium*, p. 321

Webbink, R. F., 2008, in E. F. Milone, D. A. Leahy, & D. W. Hobill, ed., Astrophysics and Space Science Library, vol. 352 of *Astrophysics and Space Science Library*, p. 233

Willems, B., Kolb, U., 2004, A&A, 419, 1057

Winget, D., Kepler, S. O., 2008, ARA&A, 46, 157

York, D. G., et al., 2000, AJ, 120, 1579

This paper has been typeset from a TEX/ LATEX file prepared by the author.